ELSEVIER

Journal of Nuclear Materials 249 (1997) 70–76

journal of nuclear materials

A new uranyl oxide hydrate phase derived from spent fuel alteration

E.C. Buck *, D.J. Wronkiewicz, P.A. Finn, J.K. Bates

Chemical Technology Division, Argonne National Laboratory, 9700 South Cass Avenue, Argonne, IL 60439-4837, USA

Received 2 April 1997; accepted 27 May 1997

Abstract

An alteration phase that formed during the corrosion of commercial oxide spent nuclear fuel has been characterized with analytical transmission electron microscopy (AEM). The phase is a Cs–Ba uranyl molybdate oxide hydrate that has an orthorhombic structure related to the alkaline earth uranyl oxide hydrates of the protasite-group minerals. On the basis of the compositional analysis and a proposed model of the structure, the ideal structural formula is $(Cs_{0.8}Ba_{0.6})(UO_2)_5(MoO_2)O_4(OH)_6 \cdot nH_2O$ (where n is around 6). Low levels of strontium are also present in the phase. The estimated unit cell parameters are $a = 0.754$ nm, $b = 0.654$ nm, and $c = 3.008$ nm. Although many of the phases formed during corrosion of spent oxide fuel are similar to those observed in natural uraninite deposits, such as Peña Blanca in Mexico, there are important differences owing to the presence of fission products in the spent fuel. Thus, accurate determination of corrosion processes in actual radioactive waste forms is important. This study suggests that the natural U–Mo deposits at Shelby, WY, and Bates Mountain Tuff, NV, may be good analogues for the long-term behavior of U–Mo phases formed due to spent fuel corrosion. © 1997 Elsevier Science B.V.

1. Introduction

The Yucca Mountain site in Nevada is being evaluated as a potential waste repository for the permanent disposal of spent nuclear fuel from commercial nuclear reactors [1]. The dissolution of spent fuel (irradiated UO_2) represents a large potential source of mobile radionuclides because of the high activity and volume of material to be buried. The dissolution kinetics of spent fuel and rates of radionuclide release are important parameters that will need to be determined before the performance of a nuclear waste repository containing spent fuel can be assessed. Uraninite (UO_2) will readily transform to the hyperstoichiometric oxide (UO_{2+x}) when exposed to oxidizing conditions [2]. In an unsaturated waste repository setting such as Yucca Mountain, water is not anticipated to be present in large amounts during the lifetime of the repository (> 10 000 years). It is more likely that water will contact the waste packages in the form of vapor and/or small amounts of dripping water. This may cause a thin film of water to form on the surface of the fuel. Under such conditions, a surface corrosion rind may form, consisting of hydrated uranyl oxide phases. Furthermore, depending on the solutes present in any water contacting the fuels, silicate, phosphate, and carbonate alteration phases may form [2,3]. Uranium oxide exposed to oxidizing conditions in the presence of simulated groundwater for 1 to 2 years formed dehydrated schoepite ($UO_3 \cdot 0.8H_2O$) and after 2 years, an assemblage of uranyl silicates developed [3]. The observed paragenic sequence (UO_2 to uranyl oxide hydrates) is similar to that observed in weathered natural uranium deposits at Shinkolobwe, Zaire, and Peña Blanca, Mexico [4,5]. As spent fuel is primarily UO_2, one might expect that it will have a closely-related paragenic sequence of alteration when exposed to similar conditions. Indeed, evidence from the testing of spent fuel (ATM-106) [6] after 3.7 years indicates the occurrence of β-uranophane and Na-boltwoodite [7], phases which have been observed at Peña Blanca [5] and in dissolution tests with UO_2 [8].

The testing of UO_2 either in the laboratory or through examination of natural uraninite deposits, has its limitations with respect to the interpretation of spent fuel alteration; namely, not all of the principal elements of concern (fission products and transuranics) are present. The behav-

* Corresponding author. Tel.: +1-630 252 6486; fax: +1-630 252 4771; e-mail: buck@cmt.anl.gov.

PII S0022-3115(97)00188-8

ior of the radioactive elements can only be properly understood if the fully radioactive waste form is tested. Radioisotopes may change the solution chemistry through radiolysis, leading to possible acidification. Radiation damage effects may also occur in the alteration phases that incorporate radionuclides. Of course, with the decay of most γ-emitters after the first 1000 years of emplacement, the γ-radiation field will be much reduced, but the α-field will remain essentially unchanged, and this effect also needs to be taken into account when testing spent fuel.

There are several uranyl oxide hydrate minerals containing different alkali and alkaline earth cations, and the extensive literature on these uranium minerals can greatly assist in their identification [9]. The large number of fission and neutron capture products present in spent fuel highlights the need for a characterization tool which both can collect structural and compositional information on the sometimes sub-micrometer alteration phases. We have used the analytical transmission electron microscope (AEM) combined with micro-manipulative techniques to accomplish this type of examination. However, the analysis of the hydrated uranyl phases from spent fuel corrosion can be particularly challenging because these phases are sensitive to electron beam irradiation. The phases tend to amorphize rapidly in the electron beam, making structural analysis difficult.

In this paper, we report on the microscopic examination of a unique alteration phase formed during dynamic testing of spent nuclear fuel. This alteration phase may control the initial solubility of some fission products that have been identified with AEM.

2. Experimental techniques

The spent nuclear fuel used in this study was approved testing material (ATM)-106 with an average burnup of 45 MWd/kg U. This oxide fuel was characterized extensively by Guenther et al. [6]. Samples of spent fuel were placed on a zircaloy retainer inside a steel test vessel. The details of the testing methodology have been presented elsewhere [3,10]. Samples of the ATM-106 spent fuel were reacted under dynamic test conditions at 90°C with a simulated groundwater leachant [10]. In these continuing dynamic tests, small amounts of a simulated groundwater (0.75 ml every 3.5 days) drips over the fuel. After 271 days, particles of altered fuel from the surface of the zircaloy retainer were removed and embedded in an epoxy resin. Electron-transparent thin sections of the reacted spent fuel alteration phases were prepared with an ultramicrotome [11]. These thin sections were laid on 200 mesh carbon-coated copper grids.

Analytical transmission electron microscopy observations were done with a JEOL 2000 FXII microscope (operated at 200 kV). Electron diffraction patterns were taken with the brightness defocused and were calibrated with known crystalline materials.

Compositional analysis was performed using X-ray energy dispersive spectroscopy (EDS) with an ultra-thin window Noran detector and by parallel electron energy-loss spectroscopy with a Gatan 666 instrument. The elemental compositions were determined with EDS within ±15% for U, Cs, and Mo. The *k*-factors for quantification were obtained from mineral standards. Electron energy-loss spectroscopy (EELS) was used to detect minor elements and to quantify the oxygen content. Microtomed thin sections of β-uranophane, $Ca[(UO_2)(SiO_3OH)]_2 \cdot 5H_2O$ and dehydrated schoepite, $UO_3 \cdot 0.8H_2O$, were used for calibration of the oxygen concentration in the unknown.

3. Results and discussion

The spent fuel alteration phases observed in this study were found to be structurally similar to but chemically distinct from minerals formed during the oxidative corrosion of uraninite and UO_2 in nature and the laboratory. The chemical differences can make comparison of spent fuel-derived alteration phases with known uraninite-weathering products unrealistic; however, models developed for performance assessment may require input of thermodynamic data from related known phases even if the actual alteration phases is unique.

To ensure representative sampling, the reacted spent fuel was examined at increasingly higher magnifications with a number of different instruments. Two types of particles were initially observed under the optical microscope. These particles included rare, black, equi-granular grains, and more commonly occurring yellow and platelet-like crystals (Fig. 1). These particles were further examined with scanning electron microscopy (SEM). In Fig. 2, an SEM image of the material on the zircaloy filter is shown. Compositional analyses of the two types of particles indicated that the black particles were composed mainly of uranium, and probably represented fine-grained

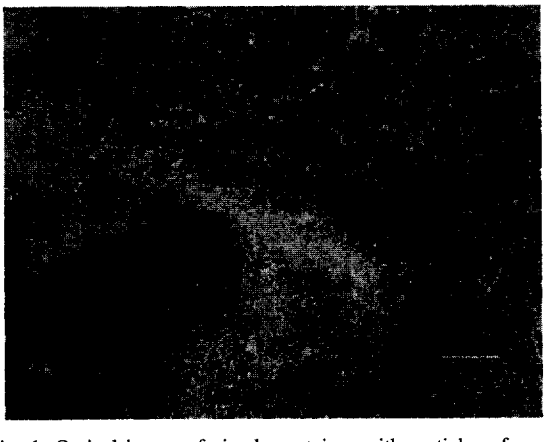

Fig. 1. Optical image of zircaloy retainer with particles of spent fuel and alteration products on the surface.

Fig. 2. Scanning electron microscopy image of a particles isolated from the zircaloy retainer. Two types of uranium-bearing phases were observed.

fragments of spent fuel. The other, which consisted of platelet-like crystals, contained U, Cs, and Mo. Samples of the latter crystals were then further examined with AEM.

3.1. Compositional analysis

The composition of the yellow platelet-like crystals was determined with both EDS and EELS. The major elements detected were U, Cs, and Mo (Fig. 3a), as determined with EDS. The spectra also indicated the presence of barium and oxygen. Based upon EDS analysis, the cation composition was determined to be $Cs_{0.5}MoU_{5.5}$. The barium and oxygen were not quantified with EDS; however, X-ray dispersive spectra generated from first principles [12] allowed the derivation of a more precise composition, $Cs_{0.75}Ba_{0.625}MoU_5$. An example of a generated X-ray spectrum is shown in Fig. 3a. The volatility of cesium was determined to be minimal during the analysis by monitoring its count-rate throughout the acquisition.

In order to increase sensitivity and visibility of EELS absorption edges, spectra were collected in second difference mode. This technique eliminates the channel-to-channel gain variation which occurs in the types of parallel detectors used in this study. The second difference EELS analysis in Fig. 3b shows only slightly different peak intensities for Ba and Cs, indicating that the phase contains nearly equal molar amounts of these elements. The electron cross-section for the U–N edges is small and, therefore the U–N edge intensity is low compared to the Cs– and Ba–M edges. The Cs–M_5 edge at 726 eV, overlaps with the U–N_5 edge, possibly due to a chemical shift of

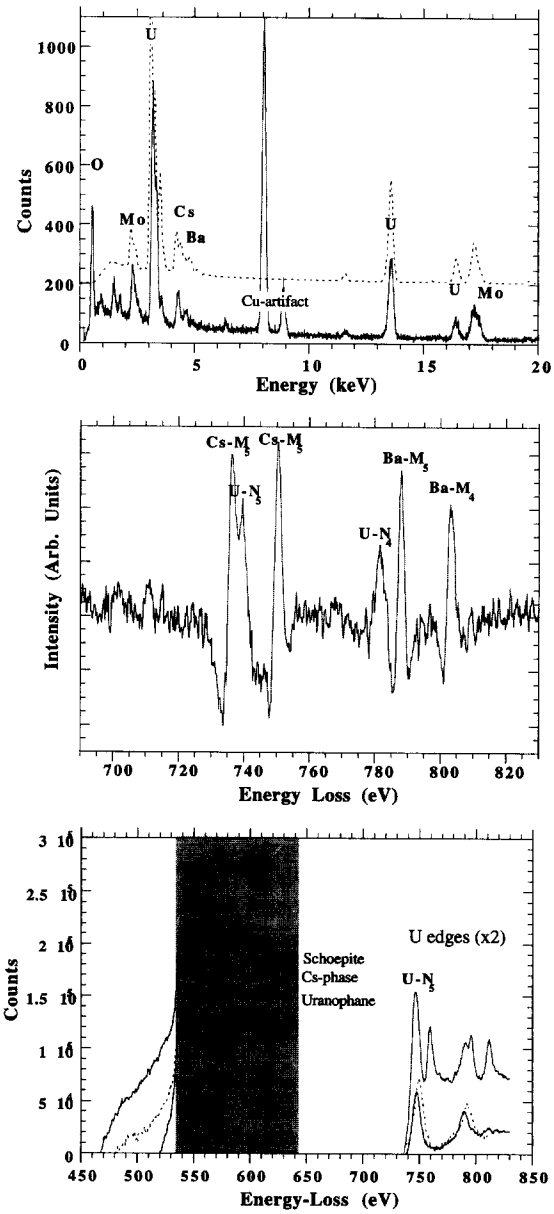

Fig. 3. (a) X-ray energy dispersive analysis of the spent fuel uranyl alteration phase. Note that only the major elements were detected: U, Mo, Cs, Ba, and O. The peaks at 1.50 ± 0.2 keV are artifacts from the specimen rod (Al) and also escape peaks of U–M X-rays. The dotted spectrum shows the calculated EDS for the phase $Cs_{0.75}Ba_{0.62}MoU_5$ (oxygen was not included in the calculation). (b) Second difference electron energy-loss spectrum of the alteration phase, showing U–$N_{4,5}$, Cs–$M_{4,5}$, and Ba–$M_{4,5}$ edges. The edge shows complex features owing to the degree of overlap and energy shifts. The U–N_5 edge has shifted about 8 eV and now overlaps with the Cs–M_5 edge. (c) Fourier-ratio deconvoluted oxygen-K edge electron energy-loss spectra of the dehydrated schoepite $[UO_3 \cdot 0.8H_2O]$, the Cs, Ba, Mo–uranyl phase, and β-uranophane, ideally $Ca[(UO_2)(SiO_3OH)]_2 \cdot 5H_2O$. Oxygen quantification was performed using the O–K edge from uranyl minerals over a 100 eV window (ΔE).

approximately 8–9 eV in the onset of the U–N-edges. Shifts in the energy of elemental absorption edges are to be expected when there is a change in the elemental speciation [13]. With EELS, we also demonstrate that the phase contains trace levels of Sr and Ru, but that the phase does not contain detectable levels of rare earth elements (REEs). Rare earths can be easily detected in the reacted spent-fuel particles [11].

Estimates of the oxygen content were made with EELS (see Fig. 3c) with a measurement of the intensities of the oxygen absorption edge from a number of uranyl minerals including the unknown alteration phase. Background-subtracted normal spectra that showed both the O–K and U–N edges were obtained with the same collection angle (~ 10 mrad) for schoepite, β-uranophane, and the Cs-bearing alteration phase. Density differences, which may be significant, between the phases were neglected, although the spectra were deconvoluted with the Fourier-ratio method to remove multiple scattering effects [13]. The counts over a 100 eV window on the O–K edge were measured for each spectrum and compared to the counts on the U–N_5 edge. As the spectra were obtained under identical conditions, the partial electron cross-sections (σ) where assumed to be the same for both the O–K and U–N edges, respectively. The analysis was performed using the following relationship:

$$\frac{N_U}{N_O} = \frac{I_N^U \sigma_K^O}{I_K^O \sigma_N^U}, \quad (1)$$

where I_K^O and I_N^U are the intensity of the O–K and U–N_5 edges respectively, and σ_K^O is the partial cross-section for the O–K edge and σ_N^U the partial cross-section for the U–N edge. Using Eq. (1) above and the following values taken under identical conditions (collection angle and sample thickness):

$$I_N^U / I_{K\,(\text{dehydrated schoepite})}^O = 0.0086, \quad (2)$$

$$I_N^U / I_{K\,(\text{uranophane})}^O = 0.0149, \quad (3)$$

the U:O ratio in dehydrated schoepite is between 1:3.75 and 1:3.9, whereas the U:O ratio is β-uranophane is 1:8.5. The I_N^U / I_K^O value determined for the Cs-bearing phase is 0.011 which suggests that the U:O ratio is around 1:4.9–6.3. Errors in the measurement come from the overlap of the Cs–M_5 edge with the U–N_5 edge and density differences between the various uranyl minerals. The overlap was resolved through deconvolution of a pure Cs–M_5 edge obtained from pollucite [$CsAlSi_2O_6$]. Based on the EDS and EELS analysis described above, the probable formula of the unknown is $Cs_{0.7\pm0.2}Ba_{0.6\pm0.2}MoU_5O_{28\pm5}$ with an uncertain amount of hydrogen.

The alteration phase from the ATM-106 fuel tests is extremely electron-beam sensitive, which suggests that the phase is hydrated. Transuranic elements were not detected with EELS in the alteration phase. The transuranics can be detected in the reacted spent fuel particles with EELS [11].

The structures of uranyl oxide hydrates are usually based upon infinite sheets of edge-sharing and corner-sharing polyhedra of higher bond valence, with low-valence cations typically located in the interlayer. The highly-charged molybdenum ion (Mo^{6+}) has a high affinity for oxygen and under oxidizing conditions will convert to a stable complex in solution (MoO_2^{2+}), with an ionic potential similar to that of dissolved UO_2^{2+} [14]. The Mo^{6+} cation occurs in a variety of coordination polyhedra in

Table 1
Measured electron diffraction parameters from the spent fuel alteration phase compared to literature X-ray diffraction parameters of synthetic billietite

d_{obs} (nm) [1]	d_{lit} (nm)	d_{cal} (nm)	
Cs, Ba Mo–uranyl phase	billietite [2]	calculated structure	*hkl*
1.500		1.504	002
0.768	0.789	0.754	100
0.753	0.753	0.752	004
0.606	0.613	0.600	012
0.576	0.570		
0.505		0.501	006
0.462	0.476	0.469	112
0.437	0.444		
0.413	0.426	0.413	114
0.390	0.389	0.398	016
0.385		0.377	200
0.374	0.376	0.376	008
0.366		0.366	202
0.345	0.350	0.352	116
0.338	0.342	0.337	204
0.333	0.332	0.336	108
0.326		0.327	020
0.321	0.321	0.320	022
0.320			
0.317	0.318		
0.303		0.301	120, 024
0.290	0.291	0.294	122
0.256	0.256	0.257	11 10
0.250		0.251	00 12
0.243		0.244	222
0.237		0.238	10 12
0.232			
0.223	0.227	0.223	11 12
0.218		0.218	030
0.215		0.216	032
0.212		0.212	316
0.205		0.204	01 14
0.198	0.197	0.199	02 12
0.189		0.189	038
0.162			

[a] Values are an average of several *d*-spacings from a number of diffraction patterns. The spacings in italics were the most common reflections observed. Errors in *d*-spacings are ±2.5%.
[b] Billietite $Ba[(UO_2)_3O_2(OH)_3]_2 \cdot 4H_2O$ has $a = 1.207$ nm, $b = 3.017$ nm, and $c = 0.714$ nm [15].

uranyl molybdate structures; tetrahedral, octahedral, and hexagonal bipyramidal [9], and in each case the Mo^{6+} cation occurs within the polyhedral sheet. The trace amount of ruthenium may behave similarly to the molybdenum in the structure, with no observable structural modifications. The low valence Cs^+ and Ba^{2+} ions probably occupy interlayer sites along with H_2O, as for all uranyl oxide hydrates [9]. The location of these species are discussed in more detail in Section 3.2.

3.2. Crystallography

The U:O ratio of the alteration phase suggests that the unknown is related to uranyl oxide hydrates that are commonly observed to form during the alteration of UO_2 in both laboratory [3] and natural [4,5] conditions. The structures of uranyl oxide hydrates have been described by Pagoaga et al. [15] and more extensively by Burns et al. [9]. In this section a possible structure for the uranyl alteration phase from the spent fuel tests is discussed. Complete structural analysis with electron diffraction of a phase containing heavy atoms, such as uranium, is not possible, owing to the large degree of multiple scattering. The methodology employed in this study is to use existing knowledge of the structures of uranyl oxide hydrates and the compositional analysis described in the previous section to develop a reasonable model of the spent fuel alteration phase. The structural model was then refined as much as possible with the available electron diffraction data. Although there are a number of uranyl minerals which contain Mo in either tetrahedral, octahedral, or hexagonal bipyramidal coordination environments, most of these were eliminated from consideration on the basis of the U:Mo ratio. For example, umohoite $[(UO_2)(MoO_4)]\cdot 4H_2O$ which consists of infinite sheets of $Ur\phi_6$ polyhedra has a U:Mo ratio of 1:1. The framework alkaline-earth uranyl ($Ur\phi_5$) molybdenum minerals (e.g., $Ba[(UO_2)_3(MoO_4)_4]\cdot 4H_2O$) has a U:Mo ratio of 3:4 [9]. The required stacking of different infinite sheets which would be necessary to obtain the composition found in the Cs-bearing alteration phase would be unprecedented for the uranyl oxide hydrates. In natural uranium minerals, both U^{4+}, and even U^{5+}, have been determined to occur in some uranyl minerals [9]. However, the severely oxidizing environment that ensue during spent fuel corrosion, probably force all released uranium into the U^{6+} state. Indeed, the oxidation potential is high enough to lead to the dissolution of the ε-ruthenium phases within the fuel [7].

The electron diffraction data from Table 1 suggest that the phase is structurally related to the becquerelite and protasite group minerals, in particular billietite $Ba[(UO_2)_3O_2(OH)_3]_2\cdot 4H_2O$, as many of the reflections are common to both the spent fuel alteration phase and to this group of uranyl oxide hydrates. The structure of billietite contains infinite sheets of edge-sharing uranyl polyhedra, with Ba^{2+} and H_2O located in the interlayer. The structure contains two distinct sheets with anion topologies, described as α-U_3O_8-type and β-U_3O_8-type [9]. The difference between these two sheets is small and depends only the position of an anion; however, the result is that one sheet contains both pentagonal bipyramids ($Ur\phi_5$ polyhedra) and square bipyramids ($Ur\phi_4$ polyhedra), whereas the other contains only $Ur\phi_5$ polyhedra.

The proposed structure was finalized with experimental and simulated diffraction patterns [16] structure using atomic coordinates for billietite published by Pagoaga et al. [15]. Single-crystal zone-axis patterns were used to provide preliminary structural data on the alteration phase. An example of an experimental electron diffraction pattern from the phase is shown in Fig. 4a. The pattern shows {002} and {006} reflections that are not observed in X-ray

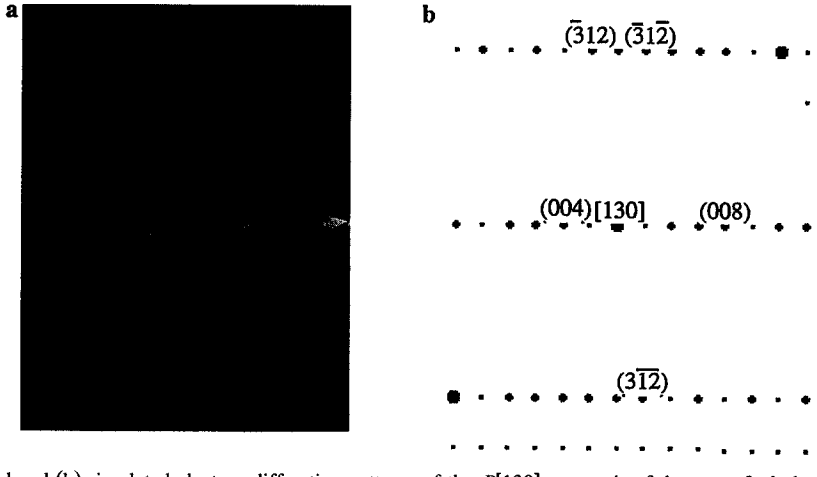

Fig. 4. (a) Experimental and (b) simulated electron diffraction patterns of the *B*[130] zone axis of the spent fuel alteration phase. Note that the diffuse halo of reflections in (a) is from nearby crystals of the alteration phase.

diffraction patterns of billietite [15]. Although the {004} reflections at around 0.75 nm are the most intense, the other reflections along the *c*-axis were also intense. This may be a consequence of stacking of uranyl–molybdenum sheets and the arrangement of the interlayer cations; however, multiple scattering may also be responsible. The diffraction pattern in Fig. 4a was indexed for the *B*[130] direction. By minimizing the sum of the squares of the residuals in the listed *d*-spacings, shown in Table 1, the unit-cell parameters were refined. A simulation of the electron diffraction pattern described earlier using these refined values is shown in Fig. 4b.

We propose that this Cs–Ba–Mo–U alteration phase, like billietite, consists of two uranyl oxide sheets, one possessing only $Ur\phi_5$ polyhedra and the other possessing both $Ur\phi_5$ polyhedra and $Ur\phi_4$ polyhedra (octahedral sites), although these latter sites may be occupied by $(MoO_2)^{2+}$ species. This results in the formation of $(UO_2)_6O_4(OH)_6$ and $(UO_2)_4(MoO_2)_2O_4(OH)_6$ sheets. The ratio of uranyl ions to oxygen (sheet) atoms is always 3:5 in the protasite-group minerals [9,15]. The fixed ratio of O to OH in the sheets is also a consequence of the nature of the sheet structure. These oxygen atoms are the ones that are not shared with the molybdenum. In Fig. 5, these are the apexes of the pentagonal bipyramidal polyhedra on the (00*l*) plane. The Cs^+ and Ba^{2+} will occupy sites between the two sheets. H_2O is also present in the interlayer, as in both becquerelite $Ca[(UO_2)_3O_2(OH)_3]_2 \cdot 8H_2O$ and the fourmarierite $Pb[(UO_2)_4O_3(OH)_4] \cdot 4H_2O$ [9,15]. The Ba^{2+} and Cs^+ ions, owing to their large size, may be coordinated by a number of H_2O groups. In the case of billietite, three H_2O molecules are coordinated around the barium ion. The H_2O molecules play a critical role in the structures of uranyl oxide hydrates, and dehydration, which can occur during exposure to the electron beam in the TEM, will result in degradation of the structure.

Based on the EDS and EELS compositional analysis and the electron diffraction analysis the proposed ideal composition is $(Cs_{0.80}Ba_{0.60})(UO_2)_5(MoO_2)O_4(OH)_6 \cdot nH_2O$ (where n is around 6) with unit-cell parameters, based on an orthorhombic lattice are: $a = 0.754 \pm 0.005$ nm, $b = 0.654 \pm 0.005$ nm, and $c = 3.008 \pm 0.001$ nm.

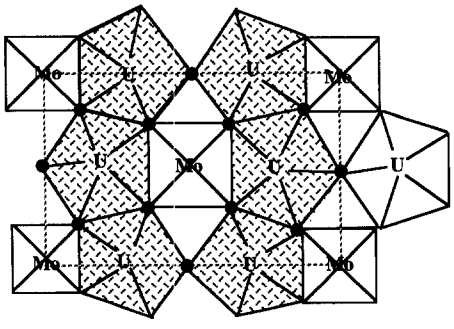

Fig. 5. Schematic of U–Mo sheet with formula $[(UO_2)_4(MoO_2)_2O_4(OH)_6]^{2-}$. The outline marks out a unit cell and within this region the oxygen atoms are represented as black dots. Hydroxide bonds will be present at the oxygen sites that are shared by the $Ur\phi_5$ polyhedra (adapted from Burns et al. [9]).

4. Further discussion

A significant proportion of the volatile elements (Cs and I), metals (Tc, Mo, and Ru), rare earths, and noble gases (Xe and Kr) present in spent fuel have been found to migrate during reactor operation and precipitate at the grain boundaries in the uranium dioxide [6,17]. The ε-phase (Mo–Ru–Tc–Pd–Rh metallic particles), which is known to form within the grains of the irradiated spent fuel [7,17], may be a source of the molybdenum that has been found in the alteration phases. We have shown that Cs, Ba, and Mo have become incorporated into this uranyl oxide hydrate alteration phase, suggesting that fission products (Cs and Mo isotopes) released during spent fuel corrosion may be isolated in discrete alteration phases.

The corrosion of spent fuel shows distinct similarities to the observed weathering of uraninite [3–5]. Although geologic analogs may provide confidence in the prediction of spent fuel durability, they may not provide all the necessary information to determine long-term behavior, as the major radioisotopes are not present. On the basis of observation of natural or laboratory-reacted UO_2, it may only be possible to speculate on the types of phases that may incorporate radionuclides.

One problem with using present-day reactor fuel to study spent fuel alteration is that many of the radioisotopes currently present in the fuel may not be present by the time the fuel begins to corrode in a geologic repository. Nevertheless, as the fission yields of ^{137}Cs ($t_{1/2} = 30.17$ yr) and ^{135}Cs ($t_{1/2} = 2.6$ Myr) are 6.2% and 2.3% respectively (calculated from Guenther et al. at a burnup of 45 MWd/kg UO_2 [6]), it is likely that a significant amount of ^{135}Cs, along with ^{137}Ba from the decay of ^{137}Cs, will always be present in the fuel and could become incorporated into alteration phases. Molybdenum, which is one of the major fission products present in ATM-106 spent fuel, can be formed through fission of uranium and beta decay of ^{95}Nb, ^{97}Nb, ^{98}Nb, and ^{100}Nb. The Mo isotopes (^{95}Mo, ^{97}Mo, ^{98}Mo, and ^{100}Mo) are stable and therefore will always be present in the fuel and ^{93}Mo ($t_{1/2} = 3500$ yr) will also be present [6]. The elements Cs, Ba, and Mo will be present in significant quantities in ATM-106. Hence, the formation of a Cs–Ba–Mo–uranyl oxide hydrate might be anticipated during long-term encapsulation of oxide fuel in a geologic repository, when weathering takes place. The formation of alteration phases during corrosion of spent fuel suggests that uranyl oxide hydrate alteration phases may retard the migration of the long-lived ^{135}Cs isotope, following its release from spent fuel.

Uranium–molybdenum deposits occur within the sandstone host rock in the Badlands of South Dakota and at outcrops at Shelby, WY, although discrete U–Mo type minerals have not been found [18]. Uranium and molybdenum mobility has also been studied at Bates Mountain Tuff in central Nevada, although precipitated U–Mo minerals were not reported [19]. The presence of a Cs–Ba–Mo–uranyl oxide alteration phases during spent fuel corrosion suggests that these natural systems warrant further investigation as possible natural analogues for spent fuel.

5. Conclusions

Testing with spent nuclear fuel under oxidizing unsaturated conditions has led to the identification of a new type of uranyl oxide hydrate phase that had not been previously identified from the study of geologic analogues. This study demonstrates the importance of performing tests with radioactive waste forms to determine possible corrosion processes that may occur during long-term disposal of spent fuel within a geologic repository. This work also suggests that natural uranium–molybdenum deposits may be relevant to the long-term behavior of some types of commercial spent nuclear fuel and that these deposits may need to be studied in greater depth.

Acknowledgements

The hot-cell work for the spent fuel tests were performed by J. Hoh and J. Emery. Thin sections of reacted spent fuel were produced by N. Dietz. This paper has benefitted from discussions with R.J. Finch. This work was performed under guidance of the Yucca Mountain Site Characterization Project (YMP) and is part of activity D-20-43 in the YMP/ Lawrence Livermore National Laboratory Spent Fuel Scientific Investigation Plan. Work supported by the U.S. Department of Energy under contract W-31-109-ENG-38.

References

[1] Site Characterization Plan, US Department of Energy, Office of Civilian Radioactive Waste Management, Report DOE/RW-0199, 1988.
[2] L.H. Johnson, D.W. Shoesmith, in: Radioactive Wasteforms for the Future, eds. W. Lutze, R.C. Ewing (Elsevier, New York, 1988) p. 665.
[3] D.J. Wronkiewicz, J.K. Bates, T.J. Gerding, E. Veleckis, B.S. Tani, J. Nucl. Mater. 192 (1992) 107.
[4] R.J. Finch, R.C. Ewing, J. Nucl. Mater. 190 (1992) 133.
[5] E.C. Pearcy, J.D. Prikryl, W.M. Murphy, B.W. Leslie, Appl. Geochem. 9 (1994) 713.
[6] R.J. Guenther, D.E. Blahnik, T.K. Campbell, U.P. Jenquin, J.E. Mendel, C.K. Thornhill, Characterization of Spent Fuel Approved Testing Material ATM-106, Pacific Northwest Laboratory Report, PNL-5109-106, 1988.
[7] P.A. Finn, J.C. Hoh, S.F. Wolf, M.T. Surchik, E.C. Buck, J.K. Bates, Scientific Basis for Nuclear Waste Management XX, Materials Research Society, Boston, MA, Dec. 2–5, 1996.
[8] D.J. Wronkiewicz, J.K. Bates, S.F. Wolf, E.C. Buck, J. Nucl. Mater. 238 (1996) 78.
[9] P.C. Burns, M.L. Miller, R.C. Ewing, Can. Mineral. 34 (1996) 845.
[10] P.A. Finn, E.C. Buck, M. Gong, J. Hoh, J. Emery, L.D. Hafenrichter, J.K. Bates, Radiochim. Acta 66-67 (1994) 189.
[11] E.C. Buck, N.L. Dietz, J.K. Bates, Annual Meeting of the Microscopy Society of America, Minneapolis, MN, Aug. 11–15, 1996, p. 562.
[12] J.I. Goldstein, D.C. Joy, Introduction to Analytical Electron Microscopy (Plenum, New York, 1979).
[13] R.F. Egerton, Electron Energy-Loss Spectroscopy (Plenum, New York, 1986).
[14] R.M. Garrels, C.L. Christ, Solutions, Minerals, and Equilibria (Harper and Row, New York, 1965).
[15] M.K. Pagoaga, D.E. Appleman, J.M. Stewart, Am. Mineral. 72 (1987) 1230.
[16] M.H. Loretto, Electron Beam Analysis of Materials (Chapman and Hall, London, 1984).
[17] L.E. Thomas, L.A. Charlot, Ceram. Trans. 9 (1990) 397.
[18] W.H. Raymond, US Geological Survey Report, OF 82-0795, Reston, VA, 1982.
[19] J.A. Kizis, MS thesis, University of Colorado (1979).